Received: 7 January 2020 | Revised: 24 March 2020 | Accepted: 27 March 2020

DOI: 10.1002/ardp.202000006

FULL PAPER

DPhG ARCH PHARM Archiv der Pharmazie

Synthesis, cytotoxicity, and molecular docking of substituted 3-(2-methylbenzofuran-3-yl)-5-(phenoxymethyl)-1,2,4-oxadiazoles

Sudhakar Mokenapelli[1] | Gangadhar Thalari[1] | Naveen Vadiyaala[1] | Jayaprakash R. Yerrabelli[1] | Vamshi K. Irlapati[2] | Neelima Gorityala[2] | Someswar R. Sagurthi[2] | Prasad R. Chitneni[1]

[1]Natural Products Laboratory, Department of Chemistry, Osmania University, Hyderabad, Telangana, India

[2]Department of Genetics and Biotechnology, Osmania University, Hyderabad, Telangana, India

Correspondence
Prasad R. Chitneni, Natural Products Laboratory, Department of Chemistry, Osmania University, Hyderabad, Telangana 500007, India.
Email: prasadraoou@yahoo.com

Funding information
University Grants Commission, Grant/Award Number: 124192

Abstract

A series of new benzofuran/oxadiazole hybrids (**8a**–**n**) was synthesized from 2*H*-chromene-3-carbonitriles (**3a**–**c**) through the multistep synthetic methodology, and these hybrids are known to exhibit anticancer activities. All the compounds were evaluated for their in vitro cytotoxicity against the HCT116 and MIA PaCa2 cell lines. Compounds **6a** (IC_{50}: 9.71 ± 1.9 μM), **6b** (IC_{50}: 7.48 ± 0.6 μM), and **6c** (IC_{50}: 3.27 ± 1.1 μM) displayed a significant cytotoxic activity, whereas compounds **8d** and **8e** exhibited good activity against both cell lines. The depletion of glycogen synthase kinase-3β (GSK3β) induces apoptosis through the inhibition of basal NF-κB activity in HCT116 colon cancer cells and MIA PaCa2 pancreatic cancer cells. Molecular docking of compounds **6a**, **6b**, **6c**, **8d**, and **8e** with GSK3β demonstrated the best binding affinity, correlating with the biological activity assay. Furthermore, the structure–activity relationship of these novel compounds reveals promising features for their use in anticancer therapy.

KEYWORDS

1, 2, 4-oxadiazole, benzofuran, cytotoxicity, docking studies, glycogen synthase kinase-3β

1 | INTRODUCTION

The benzofuran scaffold has been considered as a significant moiety in drug design and development since few years due to its progressive chemotherapeutic and physiological properties, and wide existence in nature.[1] Synthetic and natural benzofurans and its derivatives displayed numerous biological activities such as antimicrobial,[2] antibacterial,[3] anti-inflammatory,[4] antidiabetic,[5] antitumor,[6] and antineophobic activities.[7] Recently, U.S. FDA accepted drugs containing benzofuran derivatives.[8,9] Natural products with benzofuran core showed potential cytotoxicity.[10] Besides, synthetic benzofuran derivatives signify a vital source of antiproliferative agents against several tumor cell lines.[11,12] Benzofurans with substituents at C-2 and C-3 positions have been widely investigated for selective biological and pharmacological properties.[13,14] 1,2,4-Oxadiazoles are the most popular scaffolds in material science, medical chemistry, and pharmaceuticals.[15] Furthermore, the oxadiazole scaffold possesses hydrolytic, metabolic stability, and enhanced pharmacokinetic properties.[16] 1,2,4-Oxadiazoles have been defined as bioisosteres of amides and esters.[17] These are promising scaffolds of biologically active compounds, isolated from natural products.[18] Researchers mainly focused on the synthesis of 1,2,4-oxadiazole derivatives in medicinal chemistry[19] due to their remarkable biological activities, such as anticancer,[20] antibiotic,[21] antifungal,[22] antioxidant,[23] anti-inflammatory,[24] and anticonvulsant activities.[25] Recently, several 1,2,4-oxadiazole derivatives were reported having anticancer activities.[26,27] Particularly,

3,5-disubstituted-1,2,4-oxadiazoles were reported to have potential anticancer activities and apoptosis against various cancer cell lines.[28–32] These results established that 3,5-disubstituted-1,2,4-oxadiazoles are potential anticancer motifs. Herein, we designed and synthesized novel benzofuran-based 3,5-disubstituted-1,2,4-oxadiazole hybrids and evaluated their cytotoxic activities against the HCT116 (colon cancer) and MIA PaCa2 (pancreatic cancer) cell lines.

2 | RESULTS AND DISCUSSION

2.1 | Chemistry

The synthetic route of novel benzofuran-1,2,4-oxadiazole hybrids, **8a–n**, is outlined in Scheme 1. Initially, substituted salicylaldehydes **1a–c** reacted with acrylonitrile (**2**) in the presence of 1,4-diazabicyclo[2.2.2]octane (DABCO) under Baylis–Hillman reaction condition to give corresponding 2*H*-chromene-3-carbonitriles **3a–c**.[33] Sodium azide-intervened catalyst-free ring contraction reaction of compounds **3a–c** in dimethyl sulfoxide (DMSO) at 160°C temperature converted the pyran ring into the furan ring to yield 2-methylbenzofuran-3-carbonitriles **4a–c**.[34] Furthermore, compounds **4a–c** treated with hydroxylamine hydrochloride in the presence of triethylamine and ethanol at reflux temperature gave the corresponding *N*-hydroxy-2-methylbenzofuran-3-carboximidamides **5a–c**. Moreover, chloroacetyl chloride reacted with **5a–c** in tetrahydrofuran (THF) under reflux condition to yield corresponding 5-(chloromethyl)-3-(2-methylbenzofuran-3-yl)-1,2,4-oxadiazoles **6a–c**; subsequently, substituted phenols **7a–e** were treated with **6a–c** in the presence of potassium carbonate in acetone at reflux temperature to yield the corresponding 3-(2-methylbenzofuran-3yl)-5-[(substituted phenoxy)methyl]-1,2,4-oxadiazole derivatives **8a–n** in good yields. All the synthesized compounds were characterized by ^{1}H nuclear magnetic resonance (NMR), ^{13}C NMR, electrospray ionization–high-resolution mass spectrometry (ESI–HRMS), and electrospray ionization–mass spectrometry (ESI–MS).

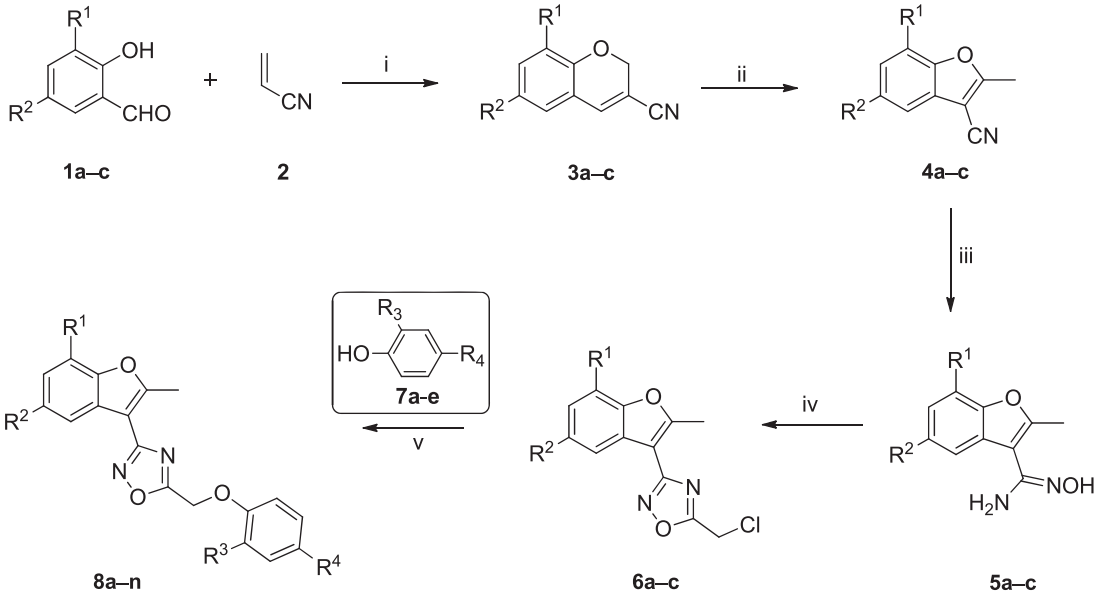

1a; **3a**; **4a**; **5a**; **6a**; R^1 = H, R^2 = H
1b; **3b**; **4b**; **5b**; **6b**; R^1 = OCH_3, R^2 = H
1c; **3c**; **4c**; **5c**; **6c**; R^1 = Br, R^2 = H

7a; R^3 = H, R^4 = H
7b; R^3 = Cl, R^4 = H
7c; R^3 = H, R^4 = Br
7d; R^3 = H, R^4 = NO_2
7e; R^3 = H, R^4 = OCH_3

8a; R^1 = H, R^2 = H, R^3 = H, R^4 = H
8b; R^1 = H, R^2 = H, R^3 = Cl, R^4 = H
8c; R^1 = H, R^2 = H, R^3 = H, R^4 = Br
8d; R^1 = H, R^2 = H, R^3 = H, R^4 = NO_2
8e; R^1 = H, R^2 = H, R^3 = H, R^4 = OCH_3
8f; R^1 = OCH_3, R^2 = H, R^3 = H, R^4 = H
8g; R^1 = OCH_3, R^2 = H, R^3 = Cl, R^4 = H
8h; R^1 = OCH_3, R^2 = H, R^3 = H, R^4 = Br
8i; R^1 = OCH_3, R^2 = H, R^3 = H, R^4 = OCH_3
8j; R^1 = H, R^2 = Br, R^3 = H, R^4 = H
8k; R^1 = H, R^2 = Br, R^3 = Cl, R^4 = H
8l; R^1 = H, R^2 = Br, R^3 = H, R^4 = Br
8m; R^1 = H, R^2 = Br, R^3 = H, R^4 = NO_2
8n; R^1 = H, R^2 = Br, R^3 = H, R^4 = OCH_3

SCHEME 1 Synthesis of compounds **8a–n**. Reagents and conditions: (i) DABCO, 80°C, 12 hr; (ii) NaN_3, DMSO, 160°C, 30 min; (iii) $NH_2OH{\cdot}HCl$, TEA, EtOH, reflux, 6 hr; (iv) chloroacetyl chloride, THF, reflux, 6 hr; (v) K_2CO_3, acetone, reflux, 1 hr. DABCO, 1,4-diazabicyclo [2.2.2]octane; DMSO, dimethyl sulfoxide; EtOH, ethyl alcohol; TEA, triethylamine; THF, tetrahydrofuran

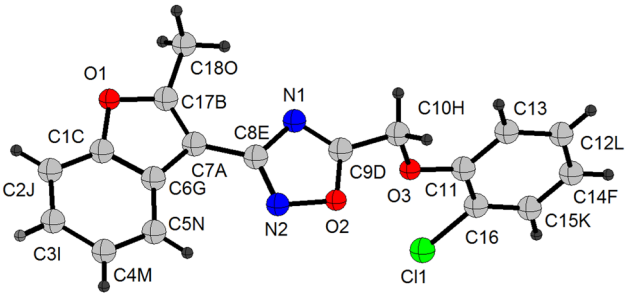

FIGURE 1 Molecular structure of compound **8b**

Furthermore, the structure of compound **8b** was confirmed by X-ray crystallography, as shown in Figure 1.

2.2 | X-ray crystallography

A single crystal was grown by the slow evaporation of the solution of compound **8b** in dichloromethane at room temperature and atmospheric pressure. The structure of **8b** was confirmed by single-crystal X-ray diffraction analysis (Figure 1). The crystallographic data of **8b** are reported in Table 1.

TABLE 1 Crystallographic data of compound **8b**

Compound	**8b**
CCDC	1991479
Formula	$C_{18}H_{13}N_2O_3Cl$
M_w	340.75
Crystal system	Triclinic
Space group	P1
T (K)	290 K
a (Å)	7.769 (3)
b (Å)	8.044 (2)
c (Å)	12.906 (4)
α (°)	85.430 (12)
β (°)	80.205 (13)
γ (°)	88.778 (12)
Z	2
V (Å^3)	792.2 (4)
D_{calc} (g/cm^3)	1.429
μ (mm^{-1})	0.260
Total reflns	4,172
Unique reflns	4,075
Observed reflns	2,713
$R_1[I > 2\sigma(I)]$	0.3048
wR_2 (all)	0.1058
GOF	1.030
Diffractometer	Bruker D8 Venture Photon III detector

Abbreviation: CCDC, Cambridge Crystallographic Data Centre; GOF, goodness of fit.

2.3 | Cytotoxic activity

All the synthesized compounds were tested for their cytotoxic activity against two cancerous cell lines, HCT116 (colon cancer) and MIA PaCa2 (pancreatic cancer). Compounds **6a**, **6b**, **6c**, **8d**, and **8e** showed <50% growth consistent with the positive control (paclitaxel), as shown in Figures 2 and 3. Comparatively, compounds **6a**, **6b**, and **6c** demonstrated notable cytotoxicity than **8d** and **8e**. IC_{50} values of all the compounds are shown in Table 2. Compounds **6a**, **6b**, **6c**, **8d**, and **8e** reported a significant cytotoxic activity, of which compound **6c** exhibited potential cytotoxicity against both cell lines.

2.4 | Molecular docking studies

Glycogen synthase kinase-3β (GSK3β) is a multifunctional serine/threonine kinase that plays a crucial role in the regulation of several signaling pathways, including cellular processes such as cell cycle, inflammation, and cell proliferation. GSK3β has been reported in the literature as one of the potential therapeutic targets for diseases such as diabetes, cancer, cardiac disease, Alzheimer's, and other central nervous system disorders.[35,36] The depletion of GSK3β induces apoptosis through the inhibition of basal NF-κB activity in HCT116 colon cancer cells[37] and MIA PaCa2 pancreatic cancer cells.[38] NF-κB activation is known to promote human cancer progression.[39] GSK3β positively regulates NF-kB binding to its target gene promoters and activates a subset of antiapoptotic (*XIAP*, *Bcl-2*) and proliferation (*cyclin D1*) genes, leading to cancer cell proliferation and survival.[40] Hence, the inhibition of GSK3β could be effective in the treatment of a wide variety of cancers. The interaction of all the synthesized compounds with GSK3β was studied by molecular docking; results are shown in Table 3. Compounds **6a–c** and **8a–n** displayed significant MolDock scores greater than −100 when docked with GSK3β (1H8F), indicating a good interaction. Conversely, compounds **6a**, **6b**, **6c**, **8d**, and **8e** exhibited potent cytotoxicity against HCT116 and MIA PaCa2 cell lines. The MolDock score, Rerank score, and interacting residues for **6a**, **6b**, **6c**, **8d**, and **8e** are listed in Table 4. Three- and two-dimensional figures are shown in Figures 4 and 5, respectively. Oxadiazole rings of **6a** and **6b** compounds form a hydrogen bond with Phe67. Furthermore, benzofuran and oxadiazole rings participate in various π interactions with Val70, Lys85, and Val87 residues. Compound **6c** formed a hydrogen bond with Asn95 and carbon–hydrogen bond with Arg96 and Glu97. π interactions were also seen with Lys85, Phe67, and Val87. In compound **8d**, hydrogen bond interactions were observed with Ser66, Asn95, and Arg96, along with carbon–hydrogen bonding with Phe67 and Glu97. Compound **8d** also displayed π bonding with Phe67, Arg96, and Glu97. Compound **8e** showed hydrogen bond interactions with amino acid residues Ser66 and Asn95, along with

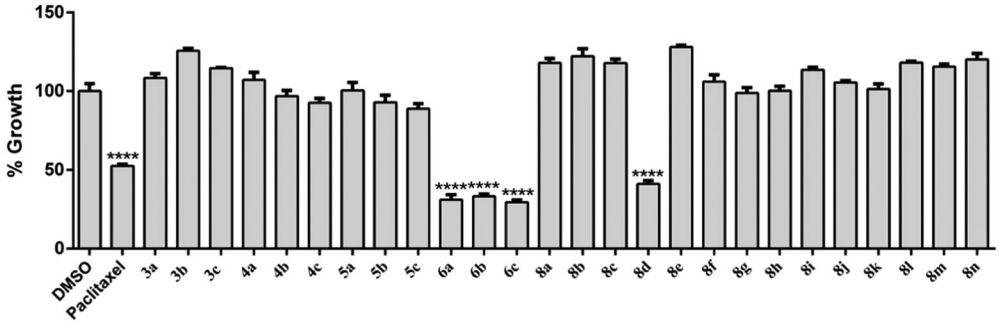

FIGURE 2 Cell proliferation of HCT116 cells 72 hr after treatment with synthesized compounds at 10-μM concentration. $p = <.0001$ indicates the significance of the data. The p value summary was represented as "****" after comparison of each test with DMSO control. DMSO, dimethyl sulfoxide

carbon–hydrogen bond interactions with Phe67, Arg96, and Glu97. Additionally, π interactions were also observed with Val87 and Arg96. All these compounds were found to have an optimum orientation with key catalytic residues such as Lys85, Glu97, and Arg96, suggesting that these hits may serve as potential cytotoxic inhibitors.

2.5 | Structure–activity relationship (SAR) studies

All the synthesized compounds were analyzed; 17 compounds displayed a significant interaction with GSK3β protein, which is revealed by a higher, negative binding free energy, as shown in Table 3. Among these synthesized derivatives, **6a**, **6b**, and **6c** showed potential cytotoxicity when tested against the HCT116 and MIA PaCa2 cell lines, in addition to compounds **8d** and **8e** that showed significant cytotoxicity against HCT116 and MIA PaCa2 cells individually. Compounds **6a**, **6b**, **6c**, **8d**, and **8e** exhibited significant IC_{50} values. Docking studies of experimentally identified compounds showed a fairly good correlation between binding free energy and IC_{50} values against GSK3β. The study reveals that compounds **6a**, **6b**, and **6c** with minimum IC_{50} values can serve as potential inhibitors, as the benzofuran ring and nitrogen of oxadiazole interact with key active site residues of an enzyme such as Lys85, Glu97, Arg96, Phe67, Val70, Val87, and Asn95. Furthermore, oxadiazole ring and chlorine interact with Lys85, which is the critical residue for the catalytic activity of the enzyme. However, **6c** showed least IC_{50} values, 3.27 and 5.34 μM in HCT116 and MIA PaCa2, respectively, due to the hydrogen bond interaction of bromine with Arg96, in addition to chlorine interaction with Lys85. Hence, electronegative group substitution of bromine at N-5 position of benzofuran ring confers enhanced activity. The phenyl substitutions of oxadiazole ring with different groups (halogen, benzyl, phenyl, and heteroaryl) have resulted in an increase and decrease of activity. In compounds **6a**, **6b**, and **6c**, the electronegative group substitution of chlorine contributed to enhanced activity, but substitution with other groups like phenoxy at the same position in compounds **8a**–**n** resulted in a decreased activity in spite of high dock scores, probably due to strong electron-withdrawing property of chlorine in compounds **6a**–**c** than phenoxyl group in compounds **8a**–**n**. However, a biological activity was observed in **8d** as the oxygen atom of oxadiazole ring and the oxygen atom of nitro group formed hydrogen bonds with the residues Asn95, Arg96, Glu97, and Ser66, respectively. In compound **8e**, oxadiazole ring and methoxy group interacted with Asn95 and Ser66 residues through hydrogen bonds. Thus, these studies reveal that oxadiazole ring upon substitution with highly electronegative atoms or heteroaryl groups imparts increased cytotoxicity. Benzofuran ring and

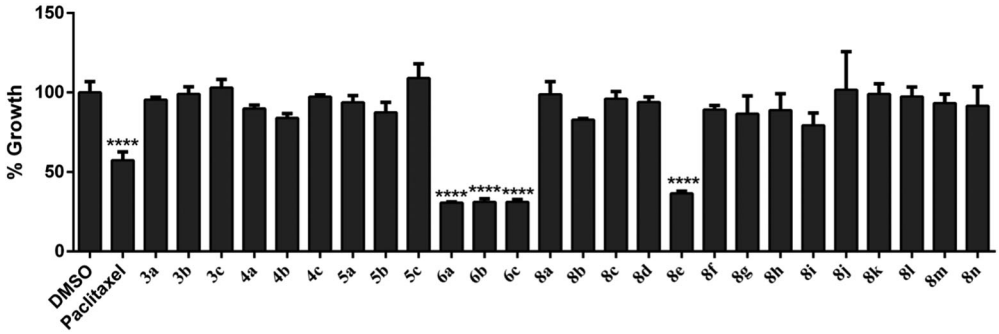

FIGURE 3 Cell proliferation of MIA PaCa2 cells 72 hr after treatment with synthesized compounds at 10-μM concentration. $p = <.0001$ indicates the significance of the data. The p value summary was represented as "****" after comparison of each test with DMSO control. DMSO, dimethyl sulfoxide

5-(chloromethyl)-3-substituted-1,2,4-oxadiazole played an important role in strengthening the interactions between synthesized derivatives and target GSK3β protein.

3 | CONCLUSION

In the present study, we developed a simple and efficient protocol for the synthesis of a novel series of benzofuran-1,2,4-oxadiazole hybrids (**8a**–**n**) from 2*H*-chromene-3-carbonitriles (**3a**–**c**) via key intermediate 2-methylbenzofuran-3-carbonitriles (**4a**–**c**). All the synthesized compounds were tested for their cytotoxicity against HCT116 and MIA PaCa2 cells. Compounds **6a**, **6b**, and **6c** demonstrated potential cytotoxicity against both cell lines, whereas compounds **8d** and **8e** exhibited significant cytotoxicity against the HCT116 and MIA PaCa2 cell lines, respectively. Furthermore, molecular docking and SAR studies explained binding affinities of benzofuran, oxadiazole, and heteroaryl rings with GSK3β protein. Thus, these results indicate that benzofuran and 3,5-disubstituted-1,2,4-oxadiazole scaffolds play a crucial role in imparting potential cytotoxicity. Further research would validate these molecules as potent anticancer agents.

TABLE 2 MTT assay in HCT116 and MIA PaCa2 cell lines after 24-hr treatment with synthesized compounds

Sl.No.	Compound	HCT116	MIA PaCa2
1	**3a**	No activity	No activity
2	**3b**	No activity	No activity
3	**3c**	No activity	No activity
4	**4a**	>100 μM	>100 μM
5	**4b**	>100 μM	>100 μM
6	**4c**	>100 μM	>100 μM
7	**5a**	No activity	No activity
8	**5b**	>100 μM	>100 μM
9	**5c**	>100 μM	>100 μM
10	**6a**	**11.27 ± 1.3 μM**	**9.71 ± 1.9 μM**
11	**6b**	**7.48 ± 0.6 μM**	**8.31 ± 0.9 μM**
12	**6c**	**3.27 ± 1.1 μM**	**5.34 ± 1.2 μM**
13	**8a**	No activity	No activity
14	**8b**	No activity	No activity
15	**8c**	No activity	No activity
16	**8d**	**11.12 ± 1.8 μM**	No activity
17	**8e**	No activity	**16.20 ± 1.7 μM**
18	**8f**	>100 μM	>100 μM
19	**8g**	>100 μM	>100 μM
20	**8h**	>100 μM	>100 μM
21	**8i**	>100 μM	>100 μM
22	**8j**	>100 μM	>100 μM
23	**8k**	No activity	No activity
24	**8l**	No activity	No activity
25	**8m**	>100 μM	>100 μM
26	**8n**	>100 μM	>100 μM
27	Paclitaxel	**3.9 μM**	**4.2 μM**

Note: Values are expressed as the mean ± standard error of the mean of three experiments. Values shown in bold possess a significant cytotoxic activity.
Abbreviation: MTT, 3-(4,5-dimethylthiazol-2-yl)-2,5-diphenyltetrazolium bromide.

TABLE 3 Molecular docking results of the compounds in chain A of glycogen synthase kinase-3β (PDB ID: 1H8F)

Ligand	MolDock score (kcal/mol)	Rerank score (kcal/mol)
Paclitaxel	−164.14	−101.40
3a	−71.03	−64.14
3b	−76.80	−67.06
3c	−74.49	−63.61
4a	−79.77	−65.71
4b	−85.08	−75.58
4c	−86.15	−70.42
5a	−85.02	−71.53
5b	−94.14	−75.30
5c	−89.36	−73.82
6a	−109.54	−85.21
6b	−113.87	−83.83
6c	−117.14	−90.03
8a	−133.82	−107.84
8b	−139.43	−109.98
8c	−130.21	−89.59
8d	−142.07	−116.79
8e	−140.79	−106.05
8f	−136.32	−106.42
8g	−143.58	−104.91
8h	−137.98	−110.09
8i	−144.12	−109.11
8j	−136.14	−97.98
8k	−134.34	−99.87
8l	−141.85	−106.44
8m	−140.26	−96.81
8n	−145.97	−118.44
8o	−137.69	−106.62

TABLE 4 Docking score results of top compounds with interacting amino acid residues in the active site of glycogen synthase kinase 3β (PDB ID:1H8F)

Ligand	MolDock score (kcal/mol)	Rerank score (kcal/mol)	Interacting residues
Paclitaxel	−164.14	−101.40	Gln185, Asp200, Lys183, Cys218
6a	−106.98	−81.47	Phe67, Val87, Lys85, Val70
6b	−113.87	−83.83	Phe67, Val87, Lys85, Val70
6c	−111.12	−79.43	Asn95, Phe67, Val87, Lys85, Glu97, Arg96
8d	−142.07	−116.79	Ser66, Phe67, Val87, Asn95, Arg96, Glu97
8e	−140.79	−106.05	Ser66, Phe67, Val87, Asn95, Arg96, Glu97

4 | EXPERIMENTAL

4.1 | Chemistry

4.1.1 | General

Unless otherwise specified, all solvents and reagents were obtained from commercial suppliers. Solvents were purified as per the procedures given in the *Textbook of Practical Organic Chemistry* by Vogel (6th edition). All reactions were performed under nitrogen atmosphere unless otherwise noted. Column chromatography was performed using Merck silica gel 60–120 mesh. NMR spectra were recorded on a Bruker Avance III spectrometer at 400 and 101 MHz. Tetramethylsilane was used as the internal standard, and chemical shift (δ) was reported in parts per million (ppm). Multiplicity of NMR signals were described as a singlet (s), doublet (d), doublet of doublet (dd), triplet of doublet (td), and multiplet (m), and coupling constant was denoted by J (in Hz). Mass spectral analysis was accomplished using electrospray ionization (ESI) technique.

The original spectra of the investigated compounds, together with their InChI keys and some biological activity data, are provided as Supporting Information Data.

4.1.2 | General procedure for the synthesis of 2*H*-chromene-3-carbonitriles (3a–c)

DABCO (1.837 g, 16.377 mmol) was added to a solution of *O*-salicylal dehyde (**1a**) (10.0 g, 81.886 mmol) in acrylonitrile (**2**) (100 ml) and stirred for 12 hr at 80°C. After completion of the reaction, the excess acrylonitrile was removed under reduced pressure, and the resultant crude product was dissolved in ethyl acetate (EtOAc; 500 ml) and washed with 5% dil. HCl. The organic layer was washed with brine solution, dried over anhydrous Na_2SO_4, purified by column chromatography using 60–120 mesh silica gel, and eluted with EtOAc/hexane (1:10) to give 2*H*-chromene-3-carbonitrile (**3a**) as a yellow solid (8.5 g).

*2H-Chromene-3-carbonitrile (**3a**)*

Yield: 65%, off-white solid, mp. 51–53°C. ^{1}H NMR (400 MHz, $CDCl_3$) δ 7.30–7.24 (m, 1H), 7.16 (s, 1H), 7.10 (dd, J = 7.5, 1.5 Hz, 1H), 6.97 (t, J = 7.5 Hz, 1H), 6.87 (d, J = 8.2 Hz, 1H), 4.80 (s, 2H). ^{13}C NMR (101 MHz, $CDCl_3$) δ 154.3, 138.8, 132.7, 128.4, 122.4, 120.0, 116.6, 116.4, 103.3, 64.3. ESI–HRMS *m/z* calcd for $C_{10}H_7NO$ 158.0606 $[M+H]^+$, found 158.0600.

*8-Methoxy-2H-chromene-3-carbonitrile (**3b**)*

Yield: 69%, yellow solid, mp. 102–104°C. ^{1}H NMR (400 MHz, $CDCl_3$) δ 7.16 (t, J = 1.3 Hz, 1H), 6.94 (d, J = 1.8 Hz, 1H), 6.92 (s, 1H), 6.74 (dd, J = 5.4, 3.7 Hz, 1H), 4.86 (s, 2H), 3.88 (s, 3H). ^{13}C NMR (101 MHz, $CDCl_3$) δ 148.0, 143.2, 138.8, 122.2, 120.7, 120.3, 116.3, 115.3, 103.4, 64.5, 56.1. ESI–HRMS *m/z* calcd for $C_{11}H_9NO_2$ 188.0711 $[M+H]^+$, found 188.0714.

*6-Bromo-2H-chromene-3-carbonitrile (**3c**)*

Yield: 63%, white solid, mp. 148–150°C. ^{1}H NMR (400 MHz, $CDCl_3$) δ 7.36 (dd, J = 8.7, 2.4 Hz, 1H), 7.23 (d, J = 2.4 Hz, 1H), 7.10 (s, 1H), 6.76 (d, J = 8.7 Hz, 1H), 4.82 (s, 2H). ^{13}C NMR (101 MHz, $CDCl_3$) δ 153.2, 137.4, 135.2, 130.6, 121.6, 118.4, 115.9, 114.4, 104.8, 64.4. ESI–HRMS *m/z* calcd for $C_{10}H_6BrNO$ 235.9711 $[M+H]^+$, found 235.9715.

4.1.3 | General procedure for the synthesis of 2-methylbenzofuran-3-carbonitriles (4a–c)

Sodium azide (3.971 g, 61.084 mmol) was added to a stirred solution of 2*H*-chromene-3-carbonitrile (**3a**) (8 g, 50.903 mmol) in DMSO (20 ml), and then the reaction mixture was heated to 160°C for 30 min. After the completion of the reaction, it was monitored by thin-layer chromatography (TLC), and the reaction mixture was quenched with ice water (200 ml) and extracted with ethyl acetate (300 ml). The organic layer was dried over anhydrous Na_2SO_4, purified by column chromatography using 60–120 mesh silica gel, and eluted with EtOAc/hexane (1:10) to give 2-methylbenzofuran-3-carbonitrile (**4a**) as a white solid (4.8 g).

*2-Methylbenzofuran-3-carbonitrile (**4a**)*

Yield: 75%, white solid, mp. 148–150°C. ^{1}H NMR (400 MHz, $CDCl_3$) δ 7.62–7.57 (m, 1H), 7.48–7.45 (m, 1H), 7.36–7.31 (m, 2H), 2.65 (s, 3H). ^{13}C NMR (101 MHz, $CDCl_3$) δ 164.8, 153.7, 125.5, 124.3, 119.5,

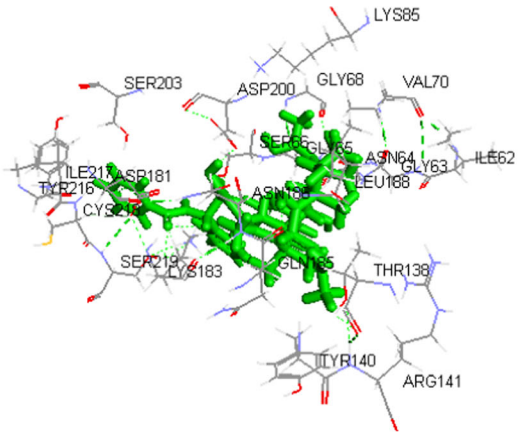

Paclitaxel

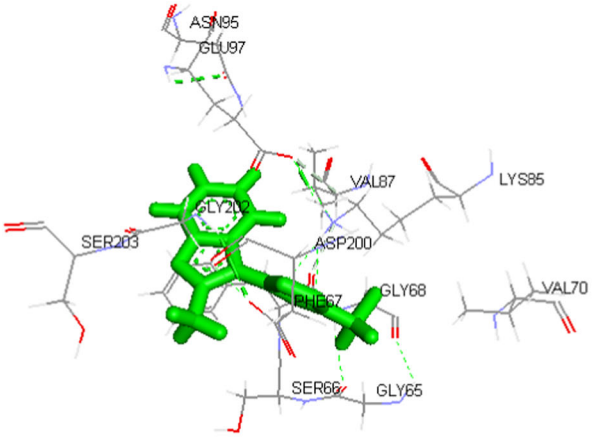

6a

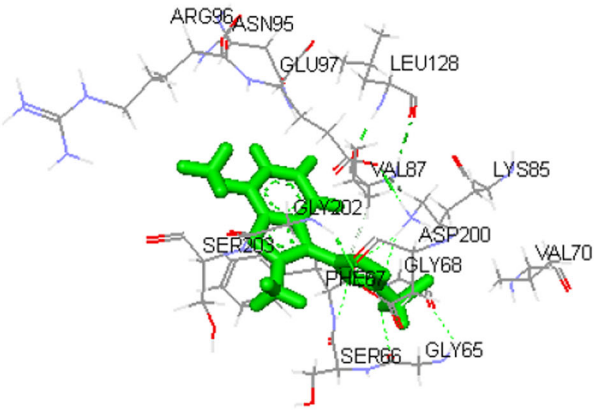

6b

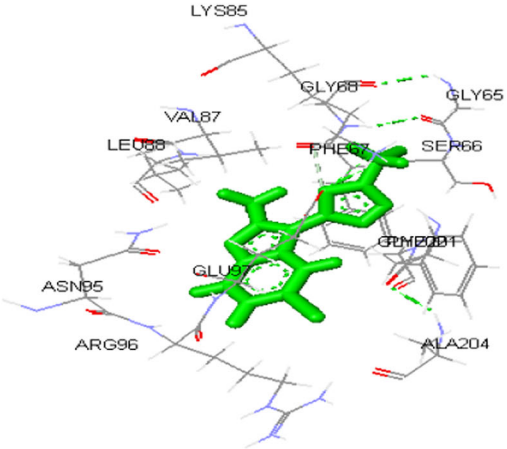

6c

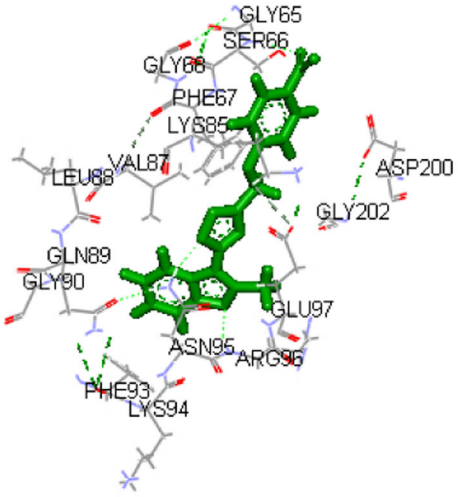

8d

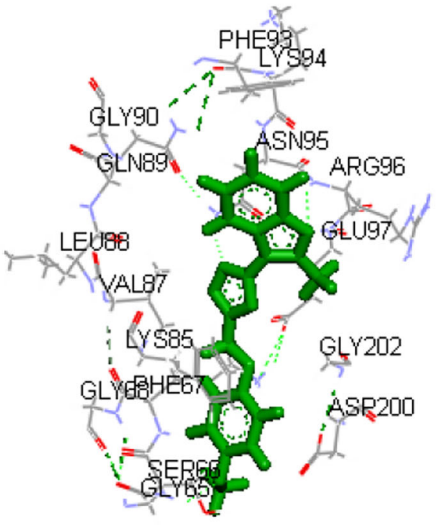

8e

FIGURE 4 Three-dimensional structure view of molecular docking of **6a**, **6b**, **6c**, **8d**, and **8e** (green sticks) with human GSK3β protein (gray lines). GSK3β, glycogen synthase kinase-3β

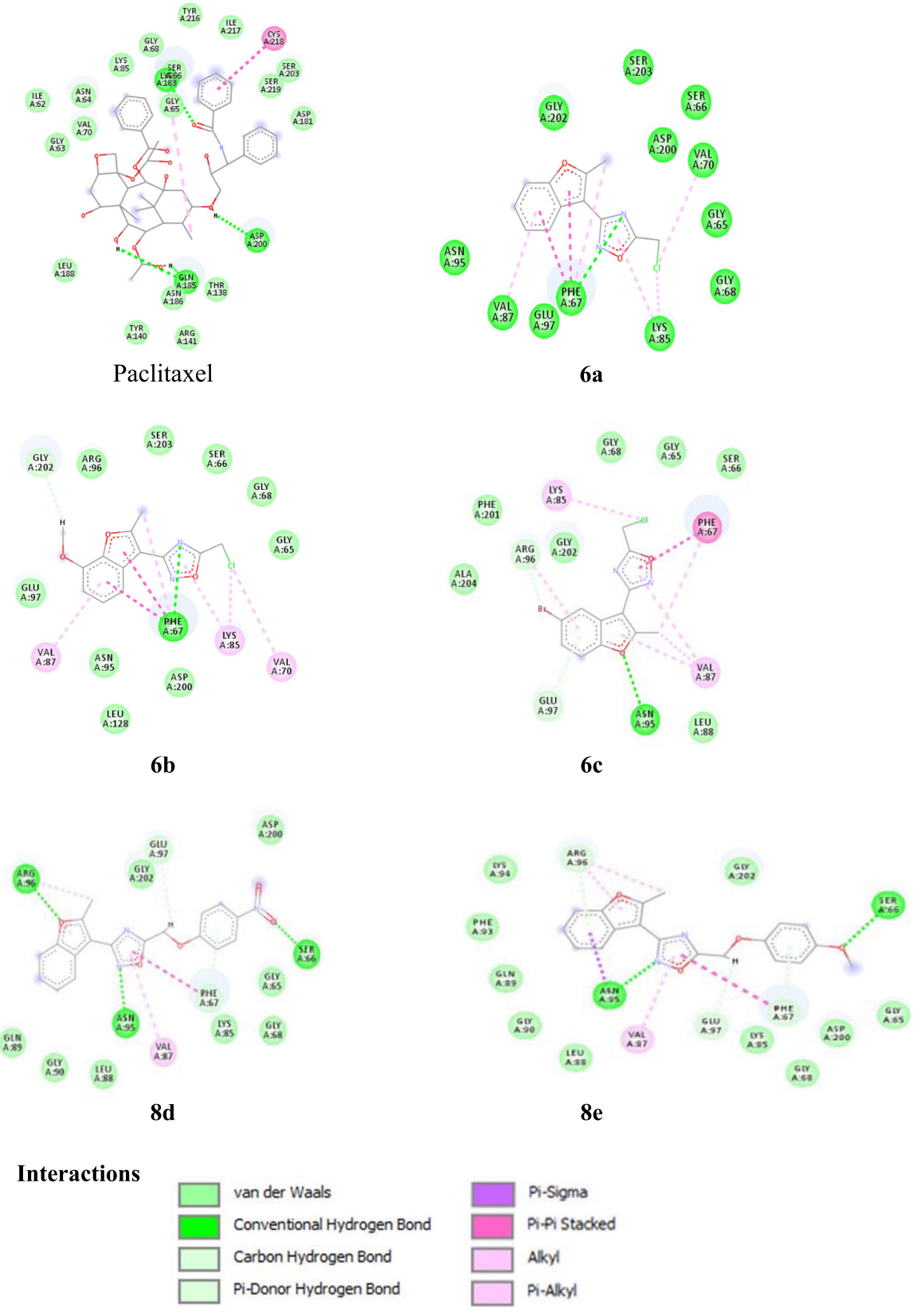

FIGURE 5 Two-dimensional receptor–ligand interactions of paclitaxel, **6a**, **6b**, **6c**, **8d**, and **8e** at the active site of the GSK3β protein. The oxadiazole ring of **6a** and **6b** shows a hydrogen bond (green dotted lines) interaction with Phe67, and the oxadiazole ring of **8d** and **8e** shows a hydrogen bond interaction with Asn95. GSK3β, glycogen synthase kinase-3β

113.3, 111.4, 91.3, 13.8. ESI–HRMS *m/z* calcd for $C_{10}H_7NO$ 158.0606 $[M+H]^+$, found 158.0600.

*7-Methoxy-2-methylbenzofuran-3-carbonitrile (**4b**)*

Yield: 56%, white solid, mp. 151–153°C. ^{1}H NMR (400 MHz, $CDCl_3$) δ 7.29–7.25 (m, 1H), 7.18 (dd, J = 7.9, 1.0 Hz, 1H), 6.86 (dd, J = 8.0, 0.9 Hz, 1H), 4.01 (s, 3H), 2.67 (s, 3H). ^{13}C NMR (101 MHz, $CDCl_3$) δ 164.7, 145.1, 127.6, 125.2, 113.3, 111.5, 107.5, 91.7, 56.1, 13.8. ESI–HRMS *m/z* calcd for $C_{11}H_9NO_2$ 188.0711 $[M+H]^+$, found 188.0715.

*5-Bromo-2-methylbenzofuran-3-carbonitrile (**4c**)*

Yield: 55%, white solid, mp. 180–182°C. ^{1}H NMR (400 MHz, $CDCl_3$) δ 7.74 (d, J = 1.9 Hz, 1H), 7.45 (dd, J = 8.8, 2.0 Hz, 1H), 7.35 (d, J = 8.7 Hz, 1H), 2.67 (s, 3H). ^{13}C NMR (101 MHz, $CDCl_3$) δ 166.0, 152.4, 128.6, 127.8, 122.3, 117.6, 112.9, 91.0, 13.9. ESI–HRMS *m/z* calcd for $C_{10}H_6BrNO$ 235.9711 $[M+H]^+$, found 235.9715.

4.1.4 | General procedure for the synthesis of *N*-hydroxy-2-methylbenzofuran-3-carboximidamides (5a–c)

A mixture of 2-methylbenzofuran-3-carbonitrile (**4a**) (4 g, 25.450 mmol), hydroxylamine hydrochloride (2.122 g, 30.540 mmol), and 10 ml of triethylamine in 50 ml of ethanol was refluxed for 6 hr. The progress of the reaction was monitored by TLC, and after the completion of the reaction, the excess ethanol and triethylamine were removed under reduced pressure. The obtained brown solid was placed in water (20 ml), and the solid precipitate was separated by filtration, washed with water, and dried at 50°C to give amidoxime as a brown solid.

N-*Hydroxy-2-methylbenzofuran-3-carboximidamide (**5a**)*

Yield: 85%, brown solid, mp. 188–190°C. ^{1}H NMR (400 MHz, $CDCl_3$) δ 7.70 (dd, J = 6.1, 2.7 Hz, 1H), 7.41 (dd, J = 6.5, 2.3 Hz, 1H), 7.26–7.22 (m, 1H), 4.92 (s, 2H), 2.61 (s, 3H). ^{13}C NMR (101 MHz, $CDCl_3$) δ 155.0, 153.8, 147.7, 126.9, 124.0, 123.1, 119.9, 110.9, 109.1, 13.6. ESI–HRMS *m/z* calcd for $C_{10}H_{10}N_2O_2$ 191.0820 $[M+H]^+$, found 191.0951.

N-*Hydroxy-7-methoxy-2-methylbenzofuran-3-carboximidamide (**5b**)*

Yield: 80%, white solid, mp. 193–195°C. ^{1}H NMR (400 MHz, $CDCl_3$) δ 7.25–7.22 (m, 2H), 6.83 (dd, J = 5.9, 2.9 Hz, 1H), 6.00 (s, 2H), 4.02 (s, 3H), 2.77 (s, 3H). ^{13}C NMR (101 MHz, $CDCl_3$) δ 166.1, 161.1, 145.2, 142.8, 127.2, 124.5, 123.8, 112.3, 111.5, 106.4, 56.0, 14.1. ESI–HRMS *m/z* calcd for $C_{11}H_{12}N_2O_3$ 221.0926 $[M+H]^+$, found 221.1008.

5-Bromo-N-*hydroxy-2-methylbenzofuran-3-carboximidamide (**5c**)*

Yield: 83%, white solid, mp. 205–207°C. ^{1}H NMR (400 MHz, $CDCl_3$) δ 7.86 (dd, J = 12.1, 1.9 Hz, 1H), 7.35 (dd, J = 8.7, 2.0 Hz, 1H), 7.27 (d, J = 3.2 Hz, 1H), 4.88 (s, 1H), 2.62 (s, 3H). ^{13}C NMR (101 MHz, $CDCl_3$) δ 156.2, 152.6, 128.8, 127.3, 126.9, 122.9, 122.4, 116.9, 116.2, 112.7, 112.3, 13.7. ESI–HRMS *m/z* calcd for $C_{10}H_9BrN_2O_2$ 268.9925 $[M+H]^+$, found 268.9989.

4.1.5 | General procedure for the synthesis of 5-(chloromethyl)-3-[(2-methylbenzofuran-3-yl)]-1,2,4-oxadiazoles (6a–c)

A mixture of *N*′-hydroxy-2-methylbenzofuran-3-carboximidamide (**5a**) (3.0 g, 15.773 mmol) in 30 ml of THF was cooled to 10°C and chloroacetyl chloride (1.50 ml, 18.927 mmol) was added dropwise; the mixture was then refluxed for 6 hr. The progress of reaction was monitored by TLC, and after the completion of the reaction, excess THF and chloroacetyl chloride were removed under reduced pressure, dissolved in ethyl acetate, and washed with water. Organic layer was dried over anhydrous Na_2SO_4, filtered, and evaporated. The crude compound was subjected to column purification with *n*-hexane to yield a colorless solid (**6a**).

*5-(Chloromethyl)-3-[(2-methylbenzofuran-3-yl)]-1,2,4-oxadiazole (**6a**)*

Yield: 65%, white solid, mp. 208–210°C. ^{1}H NMR (400 MHz, $CDCl_3$) δ 8.12–8.07 (m, 1H), 7.48–7.43 (m, 1H), 7.34–7.29 (m, 2H), 4.76 (s, 2H), 2.84 (s, 3H). ^{13}C NMR (101 MHz, $CDCl_3$) δ 173.4, 164.7, 158.8, 154.0, 126.0, 124.5, 123.6, 121.6, 110.7, 104.1, 33.3, 14.2. ESI–HRMS *m/z* calcd for $C_{12}H_9ClN_2O_2$ 249.0431 $[M+H]^+$, found 249.0437.

*5-(Chloromethyl)-3-[(7-methoxy-2-methylbenzofuran-3-yl)]-1,2,4-oxadiazole (**6b**)*

Yield: 59%, white solid, mp. 212–214°C. ^{1}H NMR (400 MHz, $CDCl_3$) δ 7.69 (dd, J = 7.9, 0.6 Hz, 1H), 7.28–7.24 (m, 1H), 6.84 (d, J = 8.0 Hz, 1H), 4.77 (s, 2H), 4.03 (s, 3H), 2.86 (s, 3H).^{13}C NMR (101 MHz, $CDCl_3$) δ 173.4, 164.6, 158.8, 144.8, 143.2, 127.6, 124.4, 113.9, 106.7, 104.5, 56.0, 33.3, 14.3. ESI–HRMS *m/z* calcd for $C_{13}H_{11}ClN_2O_3$ 279.0536 $[M+H]^+$, found 279.0543.

*3-(5-Bromo-2-methylbenzofuran-3-yl)-5-[(chloromethyl)]-1,2,4-oxadiazole (**6c**)*

Yield: 61%, white solid, mp. 215–217°C. ^{1}H NMR (400 MHz, $CDCl_3$) δ 8.23 (d, J = 2.0 Hz, 1H), 7.40 (dd, J = 8.7, 2.0 Hz, 1H), 7.31 (d, J = 8.6 Hz, 1H), 4.77 (s, 2H), 2.83 (s, 3H).^{13}C NMR (101 MHz, $CDCl_3$) δ 173.6, 164.2, 159.9, 152.8, 127.9, 127.5, 124.3, 116.8, 112.2, 103.8, 33.2, 14.3. ESI–HRMS *m/z* calcd for $C_{12}H_8BrClN_2O_2$ 326.9536 $[M+H]^+$, found 326.9543.

4.1.6 | General procedure for the synthesis of substituted 3-(2-methylbenzofuran-3-yl)-5-[(phenoxymethyl)]-1,2,4-oxadiazoles (8a–n)

A stirred solution of 5-(chloromethyl)-3-[(2-methylbenzofuran-3-yl)]-1,2,4-oxadiazole (**6a**) (0.150 g, 0.603 mmol), phenol (**7a**) (0.062 g, 0.663 mmol), and anhydrous K_2CO_3 (0.100 g, 0.723 mmol) in acetone

(20 ml) was refluxed for 1 hr. The progress of reaction was monitored by TLC, and after the completion of the reaction, acetone was removed under reduced pressure, dissolved in ethyl acetate, and washed with water (50 ml). The organic layer was dried over anhydrous Na_2SO_4, filtered, and evaporated. The crude compound was purified with column chromatography by using 5% EtOAc in *n*-hexane to yield compound **8a**.

*3-(2-Methylbenzofuran-3-yl)-5-[(phenoxymethyl)]-1,2,4-oxadiazole (**8a**)*

Yield: 81%, white solid, mp. 210–212°C. ^{1}H NMR (400 MHz, $CDCl_3$) δ 8.13–8.08 (m, 1H), 7.45 (td, J = 4.5, 3.4, 2.6 Hz, 1H), 7.35–7.28 (m, 4H), 7.07–7.01 (m, 3H), 5.35 (s, 2H), 2.83 (s, 3H). ^{13}C NMR (101 MHz, $CDCl_3$) δ 173.9, 164.4, 158.7, 157.6, 154.0, 129.7, 126.1, 124.5, 123.6, 122.3, 121.7, 114.9, 110.7, 104.2, 61.1, 14.3. ESI–HRMS *m/z* calcd for $C_{18}H_{14}N_2O_3$ 307.1082 $[M+H]^+$, found 307.1086.

*5-[(2-Chlorophenoxy)methyl]-3-[(2-methylbenzofuran-3-yl)]-1,2,4-oxadiazole (**8b**)*

Yield: 85%, white solid, mp. 210–212°C. ^{1}H NMR (400 MHz, $CDCl_3$) δ 8.12–8.08 (m, 1H), 7.48–7.44 (m, 1H), 7.42 (dd, J = 7.9, 1.6 Hz, 1H), 7.33–7.29 (m, 2H), 7.24–7.20 (m, 1H), 7.09 (dd, J = 8.3, 1.3 Hz, 1H), 7.00 (td, J = 7.7, 1.4 Hz, 1H), 5.44 (s, 2H), 2.84 (s, 3H). ^{13}C NMR (101 MHz, $CDCl_3$) δ 173.4, 164.4, 158.7, 154.0, 153.3, 130.8, 127.8, 126.0, 124.5, 123.9, 123.6, 123.4, 121.6, 115.0, 110.7, 104.1, 62.3, 14.3. ESI–HRMS *m/z* calcd for $C_{18}H_{13}ClN_2O_3$ 341.0693 $[M+H]^+$, found 341.0698.

*5-[(4-Bromophenoxy)methyl]-3-[(2-methylbenzofuran-3-yl)]-1,2,4-oxadiazole (**8c**)*

Yield: 88%, white solid, mp. 215–217°C. ^{1}H NMR (400 MHz, $CDCl_3$) δ 8.11–8.07 (m, 1H), 7.48–7.40 (m, 3H), 7.34–7.30 (m, 2H), 6.95–6.91 (m, 2H), 5.34 (s, 2H), 2.83 (s, 3H). ^{13}C NMR (101 MHz, $CDCl_3$) δ 173.4, 164.4, 158.7, 156.7, 154.0, 132.6, 126.0, 124.5, 123.6, 121.6, 116.8, 114.7, 110.7, 104.1, 61.2, 14.3. ESI–HRMS *m/z* calcd for $C_{18}H_{13}BrN_2O_3$ 385.0188 $[M+H]^+$, found 385.0201.

*3-(2-Methylbenzofuran-3-yl)-5-[(4-nitrophenoxy)methyl]-1,2,4-oxadiazole (**8d**)*

Yield: 65%, white solid, mp. 208–210°C. ^{1}H NMR (400 MHz, $CDCl_3$) δ 8.28–8.22 (m, 2H), 8.10–8.06 (m, 1H), 7.50–7.44 (m, 1H), 7.35–7.30 (m, 2H), 7.16–7.10 (m, 2H), 5.47 (s, 2H), 2.83 (s, 3H). ^{13}C NMR (101 MHz, $CDCl_3$) δ 172.5, 164.5, 162.1, 158.8, 154.0, 142.7, 126.0, 124.6, 123.7, 121.5, 114.9, 110.8, 104.0, 61.1, 14.3. ESI–HRMS *m/z* calcd for $C_{18}H_{13}N_3O_5$ 352.0963 $[M+H]^+$, found 352.0984.

*5-[(4-Methoxyphenoxy)methyl]-3-(2-methylbenzofuran-3-yl)-1,2,4-oxadiazole (**8e**)*

Yield: 75%, white solid, mp. 207–209°C. ^{1}H NMR (400 MHz, $CDCl_3$) δ 8.10 (s, 2H), 7.44 (s, 2H), 7.11 (d, J = 7.6 Hz, 2H), 6.93 (d, J = 7.9 Hz, 2H), 5.32 (s, 2H), 4.74 (s, 3H), 2.83 (s, 3H). ^{13}C NMR (101 MHz, $CDCl_3$) δ 174.0, 173.4, 164.7, 164.3, 158.7, 158.6, 154.0, 130.1, 124.5, 124.4, 123.6, 123.5, 121.7, 121.6, 114.9, 110.7, 110.7, 104.3, 61.4, 33.3, 14.2. ESI–HRMS *m/z* calcd for $C_{19}H_{16}N_2O_4$ 337.1188 $[M+H]^+$, found 337.1196.

*3-(7-Methoxy-2-methylbenzofuran-3-yl)-5-(phenoxymethyl)-1,2,4-oxadiazole (**8f**)*

Yield: 80%, white solid, mp. 205–207°C. ^{1}H NMR (400 MHz, $CDCl_3$) δ 7.70 (d, J = 8.4 Hz, 1H), 7.36–7.30 (m, 2H), 7.27–7.24 (m, 1H), 7.07–7.01 (m, 3H), 6.84 (d, J = 7.9 Hz, 1H), 5.37 (s, 2H), 4.02 (s, 3H), 2.86 (s, 3H). ^{13}C NMR (101 MHz, $CDCl_3$) δ 173.9, 164.3, 158.7, 157.6, 144.8, 129.7, 127.7, 124.3, 122.3, 114.9, 113.9, 106.6, 104.6, 61.1, 56.0, 14.3. ESI–HRMS *m/z* calcd for $C_{19}H_{16}N_2O_4$ 337.1188 $[M+H]^+$, found 337.1196.

*5-[(2-Chlorophenoxy)methyl]-3-(7-methoxy-2-methylbenzofuran-3-yl)-1,2,4-oxadiazole (**8 g**)*

Yield: 84%, white solid, mp. 209–211°C. ^{1}H NMR (400 MHz, $CDCl_3$) δ 7.69 (d, J = 7.9 Hz, 1H), 7.41 (d, J = 7.2 Hz, 1H), 7.27–7.20 (m, 2H), 7.09 (d, J = 8.0 Hz, 1H), 7.00 (t, J = 7.4 Hz, 1H), 6.83 (d, J = 7.9 Hz, 1H), 5.43 (s, 2H), 4.02 (s, 3H), 2.85 (s, 3H). ^{13}C NMR (101 MHz, $CDCl_3$) δ 173.4, 164.3, 158.7, 153.3, 144.8, 143.2, 130.8, 127.8, 124.3, 123.46, 115.0, 113.9, 106.7, 104.6, 62.2, 56.0, 14.3. ESI–HRMS *m/z* calcd for $C_{19}H_{15}ClN_2O_4$ 371.0798 $[M+H]^+$, found 371.0806.

*5-[(4-Bromophenoxy)methyl]-3-(7-methoxy-2-methylbenzofuran-3-yl)-1,2,4-oxadiazole (**8h**)*

Yield: 88%, white solid, mp. 212–214°C. ^{1}H NMR (400 MHz, $CDCl_3$) δ 7.68 (dd, J = 7.8, 0.6 Hz, 1H), 7.45–7.40 (m, 2H), 7.25 (dd, J = 10.2, 5.7 Hz, 1H), 6.96–6.90 (m, 2H), 6.84 (d, J = 7.8 Hz, 1H), 5.34 (s, 2H), 4.03 (s, 3H), 2.85 (s, 3H). ^{13}C NMR (101 MHz, $CDCl_3$) δ 173.4, 164.4, 158.7, 156.7, 144.8, 132.6, 127.7, 124.4, 116.8, 113.9, 106.7, 104.5, 61.2, 56.0, 14.3. ESI–HRMS *m/z* calcd for $C_{19}H_{15}BrN_2O_4$ 415.0293 $[M+H]^+$, found 415.0298.

*3-(7-Methoxy-2-methylbenzofuran-3-yl)-5-[(4-methoxyphenoxy)-methyl]-1,2,4-oxadiazole (**8i**)*

Yield: 70%, white solid, mp. 212–214°C. ^{1}H NMR (400 MHz, $CDCl_3$) δ 7.69 (dd, J = 7.9, 0.7 Hz, 1H), 7.27–7.23 (m, 1H), 7.11 (d, J = 8.3 Hz, 2H), 6.95–6.92 (m, 2H), 6.83 (d, J = 7.8 Hz, 1H), 5.33 (s, 2H), 4.02 (s, 3H), 2.85 (s, 3H). ^{13}C NMR (101 MHz, $CDCl_3$) δ 174.1, 164.3, 158.6, 155.6, 144.7, 143.2, 131.7, 130.1, 127.7, 124.3, 114.8, 113.9, 106.6, 104.7, 61.3, 56.0, 20.5, 14.3. ESI–HRMS *m/z* calcd for $C_{20}H_{18}N_2O_5$ 367.1294 $[M+H]^+$, found 367.1298.

*3-(5-Bromo-2-methylbenzofuran-3-yl)-5-(phenoxymethyl)-1,2,4-oxadiazole (**8j**)*

Yield: 84%, white solid, mp. 208–210°C. ^{1}H NMR (400 MHz, $CDCl_3$) δ 8.24 (d, J = 2.0 Hz, 1H), 7.40 (dd, J = 8.7, 2.0 Hz, 1H), 7.36–7.30 (m, 3H), 7.07–7.02 (m, 3H), 5.38 (s, 2H), 2.83 (s, 3H). ^{13}C NMR (101 MHz, $CDCl_3$) δ 174.1, 163.9, 159.8, 157.5, 152.8, 129.7, 128.0, 127.4, 124.4, 122.4, 116.8, 114.9, 112.2, 103.9, 61.0, 14.3. ESI–HRMS *m/z* calcd for $C_{18}H_{13}BrN_2O_3$ 385.0188 $[M+H]^+$, found 385.0193.

*3-(5-Bromo-2-methylbenzofuran-3-yl)-5-[(2-chlorophenoxy)methyl]-1,2,4-oxadiazole (**8k**)*

Yield: 87%, white solid, mp. 212–214°C. ^{1}H NMR (400 MHz, $CDCl_3$) δ 8.23 (d, J = 2.0 Hz, 1H), 7.45–7.38 (m, 2H), 7.31 (d, J = 8.6 Hz, 1H), 7.25 (td, J = 8.3, 6.1, 1.6 Hz, 1H), 7.10 (dd, J = 8.3, 1.3 Hz, 1H), 7.01 (td, J = 7.7, 1.3 Hz, 1H), 5.45 (s, 2H), 2.82 (s, 3H). ^{13}C NMR (101 MHz, $CDCl_3$) δ 173.6, 163.9, 159.9, 152.8, 130.8, 127.8, 127.4, 124.3, 123.5, 116.8, 115.0, 112.2, 103.8, 62.2, 14.3. ESI–HRMS *m/z* calcd for $C_{18}H_{12}BrClN_2O_3$ 418.9798 $[M+H]^+$, found 418.9803.

*3-(5-Bromo-2-methylbenzofuran-3-yl)-5-[(4-bromophenoxy)methyl]-1,2,4-oxadiazole (**8l**)*

Yield: 84%, white solid, mp. 215–217°C. ^{1}H NMR (400 MHz, $CDCl_3$) δ 8.22 (d, J = 2.0 Hz, 1H), 7.44–7.40 (m, 2H), 7.39 (d, J = 2.0 Hz, 1H), 7.33–7.29 (m, 1H), 6.95–6.91 (m, 2H), 5.34 (s, 2H), 2.81 (s, 3H). ^{13}C NMR (101 MHz, $CDCl_3$) δ 173.6, 163.9, 159.9, 156.6, 152.8, 132.6, 127.9, 127.4, 124.3, 116.8, 114.8, 112.2, 103.8, 61.2, 14.3. ESI–HRMS *m/z* calcd for $C_{18}H_{12}Br_2N_2O_3$ 462.9293 $[M+H]^+$, found 462.9298.

*3-(5-Bromo-2-methylbenzofuran-3-yl)-5-[(4-nitrophenoxy)methyl]-1,2,4-oxadiazole (**8m**)*

Yield: 73%, white solid, mp. 212–214°C. ^{1}H NMR (400 MHz, $CDCl_3$) δ 8.28–8.24 (m, 2H), 8.21 (d, J = 1.9 Hz, 1H), 8.15 (d, J = 9.1 Hz, 1H), 7.41 (dd, J = 8.7, 2.0 Hz, 1H), 7.17–7.12 (m, 2H), 5.49 (s, 2H), 2.82 (s, 3H). ^{13}C NMR (101 MHz, $CDCl_3$) δ 172.8, 164.0, 162.1, 160.0, 152.8, 142.7, 127.8, 127.5, 126.2, 126.0, 116.9, 115.6, 114.9, 103.7, 61.1, 14.3. ESI–HRMS *m/z* calcd for $C_{18}H_{12}BrN_3O_5$ 430.0038 $[M+H]^+$, found 430.0045.

*3-(5-Bromo-2-methylbenzofuran-3-yl)-5-[(4-methoxyphenoxy)-methyl]-1,2,4-oxadiazole (**8n**)*

Yield: 86%, white solid, mp. 209–211°C. ^{1}H NMR (400 MHz, $CDCl_3$) δ 8.25 (d, J = 2.0 Hz, 1H), 7.40 (dd, J = 8.7, 2.0 Hz, 1H), 7.31 (d, J = 8.7 Hz, 1H), 7.13 (d, J = 8.2 Hz, 2H), 6.98–6.92 (m, 2H), 5.35 (s, 2H), 2.83 (s, 3H), 2.30 (s, 3H). ^{13}C NMR (101 MHz, $CDCl_3$) δ 174.3, 163.8, 159.8, 155.5, 152.8, 131.8, 130.1, 127.4, 124.4, 116.8, 114.9, 112.1, 103.9, 61.3, 20.5, 14.3. ESI–HRMS *m/z* calcd for $C_{19}H_{15}BrN_2O_4$ 413.0293 $[M+H]^+$, found 413.0298.

4.2 | Biology

4.2.1 | Maintenance of cell line model systems

In this study, two cancer cell lines were used, namely HCT116 and MIA PaCa2, which represent colon and pancreatic cancers, respectively. Both the cell lines were maintained as monolayer cultures and continuously observed under phase-contrast microscope to ensure contamination-free cells. The cell lines were grown in Dulbecco's modified Eagles's medium supplemented with 10% (v/v) of fetal bovine serum and 1× concentration of PenStrep antibiotic (Gibco). The cells were maintained in 5% CO_2 incubator supplemented with 37°C humidification.[41]

4.2.2 | Cytotoxic assay

MTT assay (3-[4,5-dimethylthiazol-2-yl]-2,5-diphenyltetrazolium bromide) was used to determine the cell proliferation of the cell lines after treatment with test compounds.[42] The log-phase cells were trypsinized, counted, and seeded into 96-well plates in predetermined numbers on the basis of the cell line type. After 24 hr of recovery period, the cells were treated with test compounds at a final concentration of 10 μM along with DMSO control and positive control (paclitaxel). The treated cells were processed after 72 hr endpoint by adding 40-μl MTT solution (5 mg/ml stock prepared in phosphate-buffered saline). Incubated for 2 hr at 37°C in CO_2 incubator, followed by centrifugation at 500*g* for 5 min and aspiration of the growth media, 200 μl of DMSO was added to each well to solubilize the insoluble purple formazan crystals that were formed due to cleavage of MTT by cellular mitochondrial dehydrogenases. The plates were subjected to shaking on a plate shaker to ensure complete solubilization. The final absorbance was read at 540 nm with a reference filter of 690 nm. The percentage cell viability or % growth was determined relative to DMSO control. IC_{50} values were generated using 5-dose treatment and finally analyzed with GraphPad Prism version 6.0.

4.3 | Docking studies

The interaction of GSK3β protein with substituted 3-(2-methylbenzofuran-3-yl)-5-(phenoxymethyl)-1,2,4-oxadiazoles was studied using Molegro Virtual Docker (MVD 2012.5.5).[43] Docking was performed at the potential active site of GSK3β protein with synthesized derivatives and paclitaxel. The structures of all the synthesized compounds were generated using MarvinSketch 5.6.0.2. (1998–2011, Copyright © ChemAxon Ltd.), cleaned in 3D, and saved in .pdb format for docking studies. The PDB file of the target protein was downloaded from RCSB PDB (www.rcsb.org), GSK3β (PDB ID:1H8F). During docking, the protein and ligands were prepared by assigning bonds, bond orders, charges, explicit hydrogen, and flexible torsions in ligands if they were missing. The search algorithm was taken as MolDock SE and the number of runs was taken as 10; maximum iterations were 2,000, with a population size of 50 and with an energy threshold of 100. Further investigations of the binding interactions of the most active docked compounds were performed using BIOVIA Discovery Studio 2017 R2 Client. To obtain more potent compounds as inhibitors, the optimal binding mode of a molecule to the active site of macromolecule was interpreted.

ACKNOWLEDGMENTS

Sudhakar Mokenapelli acknowledges UGC, New Delhi, India, for providing UGC-SRF fellowship, head of Department of Chemistry and CFRD Osmania University, Hyderabad, India, for providing facilities and Advanced Centre of Research in High Energy Materials (ACRHEM), and the University of Hyderabad for X-ray crystallography facility.

CONFLICT OF INTERESTS

The authors declare that there are no conflicts of interests.

ORCID

Sudhakar Mokenapelli http://orcid.org/0000-0001-9575-4830
Jayaprakash R. Yerrabelli http://orcid.org/0000-0003-4387-8334
Someswar R. Sagurthi http://orcid.org/0000-0003-1939-0849
Prasad R. Chitneni http://orcid.org/0000-0003-0062-9856

REFERENCES

[1] H. Khanam, *Eur. J. Med. Chem.* **2015**, *97*, 483.
[2] M. Koca, S. Servi, C. Kirilmis, M. Ahmedzade, C. Kazaz, B. Ozbek, G. Otuk, *Eur. J. Med. Chem.* **2005**, *40*, 1351.
[3] G. K. Rao, K. N. Venugopala, P. N. S. Pai, *J. Pharmacol. Toxicol.* **2007**, *2*, 481.
[4] K. M. Dawood, H.-G. Abdel, E. A. Rageb, M. Ellithey, H. A. Mohamed, *Bioorg. Med. Chem.* **2006**, *14*, 3672.
[5] K. Tsujihara, M. Hongu, K. Saito, H. Kawanishi, K. Kuriyama, M. Matsumoto, A. Oku, K. Ueta, M. Tsuda, A. Saito, *J. Med. Chem.* **1999**, *42*, 5311.
[6] L. Pieter, S. V. Dyck, M. Gao, R. Bai, E. Hamel, A. Vlietinck, G. Lemiere, *J. Med. Chem.* **1999**, *42*, 5475.
[7] Y. Liao, A. P. Kozikowski, A. Guidotti, E. Costa, *Bioorg. Med. Chem. Lett.* **1998**, *8*, 2099.
[8] D. D. Michael, T. S. David, B. J. Anderson, J. T. Njardarson, *J. Med. Chem.* **2018**, *61*, 10996.
[9] A. Radadiya, A. Shah, *Eur. J. Med. Chem.* **2015**, *97*, 356.
[10] A. H. Banskota, Y. Tezuka, K. Midorikawa, K. Matsushige, S. Kadota, *J. Nat. Prod.* **2000**, *63*, 1277.
[11] I. Hayakawa, R. Shioya, T. Agatsuma, H. Furukawa, S. Narutocand, Y. Sugano, *Bioorg. Med. Chem. Lett.* **2004**, *14*, 455.
[12] M. Hranjec, I. Sovic, I. Ratkaj, G. Pavlovic, N. Ilic, L. Valjalo, K. Pavelic, S. Kraljevic, G. Pavelic, Z. Karminski, *Eur. J. Med. Chem.* **2013**, *69*, 823.
[13] K. Manna, Y. K. Agarwal, *Bioorg. Med. Chem. Lett.* **2009**, *19*, 2688.
[14] A. Hall, A. Billinton, S. H. Brown, N. M. Clayton, A. Chowdhury, G. M. P. Giblin, P. Goldsmith, T. G. Hayhow, D. N. Hurst, I. R. Kilford, A. Naylor, B. Passingham, L. Winyard, *Bioorg. Med. Chem. Lett.* **2008**, *18*, 3392.
[15] (a) A. Pace, P. Pierro, *Org. Biomol. Chem.* **2009**, *7*, 4337; (b) J. Bostrom, A. Hogner, A. Llinas, E. Wellner, A. T. Plowright, *J. Med. Chem.* **2012**, *55*, 1817; (c) N. P. Rai, V. K. Narayanaswamy, T. Govender, B. K. Manuprasad, S. Shashikanth, P. N. Arunachalam, *Eur. J. Med. Chem.* **2010**, *45*, 2677; (d) H. Z. Zhang, S. Kasibhatla, J. Kuemmerle, W. Kemnitzer, K. Ollis-Mason, L. Qiu, C.-G. Crogan, B. Tseng, J. Drewe, S. X. Cai, *J. Med. Chem.* **2005**, *48*, 5215; (e) Y. J. Chen, S. C. Yang, C. C. Tsai, K. C. Chang, W. H. Chuang, W. L. Chu, V. Kovalev, W. S. Chung, *Chem. Asian J.* **2015**, *10*, 1025.
[16] L. B. Clapp, *Adv. Heterocycl. Chem.* **1976**, *13*, 65.
[17] K. E. Andersen, A. S. Jorgensen, C. Braestrup, *Eur. J. Med. Chem.* **1994**, *29*, 393.
[18] J. C. Jochims, A. R. Katritzky, C. W. Rees, E. V. F. Scriven, *Heterocycl. Chem. II* **1996**, *4*, 179.
[19] A. Vaidya, S. Jain, P. Jain, *Mini Rev. Med. Chem.* **2016**, *16*, 825.
[20] D. Kumar, G. Patel, A. K. Chavers, K. H. Chang, K. Shah, *Eur. J. Med. Chem.* **2011**, *46*, 3085.
[21] E. Spink, D. Ding, Z. Peng, *J. Med. Chem.* **2015**, *58*, 1380.
[22] J. N. Sangshetti, D. B. Shinde, *Eur. J. Med. Chem.* **2011**, *46*, 1040.
[23] J. G. Leal, A. C. Sauer, J. C. P. Mayer, *New J. Chem.* **2017**, *41*, 5875.
[24] M. Farooqui, R. Bora, C. R. Patil, *Eur. J. Med. Chem.* **2009**, *44*, 794.
[25] M. M. Khanaposhtani, M. Shabani, M. Faizi, *Eur. J. Med. Chem.* **2016**, *112*, 91.
[26] W. Kemnitzer, J. Kuemmerle, H. Z. Zhang, *Bioorg. Med. Chem. Lett.* **2009**, *19*, 4410.
[27] J. Cai, H. Wei, K. H. Hong, *Eur. J. Med. Chem.* **2015**, *96*, 1.
[28] J. Matsumoto, T. Takahashi, M. Agata, H. Toyofuku, N. Sasada, *Jpn. J. Pharmacol.* **1994**, *65*, 51.
[29] H. Z. Zhang, S. Kasibhatla, J. Kuemmerle, W. Kemnitzer, K. Ollis-Mason, L. Qiu, C. Crogan-Grundy, B. Tseng, J. Drewe, S. X. Cai, *J. Med. Chem.* **2005**, *48*, 5215.
[30] J. V. Dos Anjos, N. Filho RAW, S. C. Do Nascimento, R. M. Srivastava, S. J. De Melo, D. Sinou, *Eur. J. Med. Chem.* **2009**, *44*, 3571.
[31] W. Kemnitzer, J. Kuemmerle, H. Z. Zhang, S. Kasibhatla, B. Tseng, J. Drewe, S. X. Cai, *Bioorg. Med. Chem. Lett.* **2009**, *19*, 4410.
[32] D. Kumar, G. Patel, E. O. Johnson, K. Shah, *Bioorg. Med. Chem. Lett.* **2009**, *19*, 2739.
[33] K. S. Kumar, V. Daniel, S. K. Shanker, C. P. Rao, G. L. D. Krupadanam, *Med. Chem. Res.* **2016**, *25*, 2179.
[34] S. D. Gawande, M. J. Raihan, M. R. Zanwar, K. Veerababurao, D. Janreddy, C. W. Kuo, M. L. Chen, T. S. Kuo, C. F. Yao, *Tetrahedron* **2013**, *69*, 1841.
[35] S. Phukan, V. S. Babu, A. Kannoji, R. Hariharan, V. N. Balaji, *Br. J. Pharmacol.* **2010**, *160*, 1.
[36] H. Ernst ter, T. C. Joyce, A. A. Douglas, H. Hsun-Mei, L. Swenson, J. Jugnu, *Nat. Struct. Mol. Biol.* **2001**, *8*, 593.
[37] A. Shakoori, A. Ougolkov, Z. W. Yu, B. Zhang, M. H. Modarressi, D. D. Billadeau, M. Mai, Y. Takahashi, T. Minamoto, *Biochem. Biophys. Res. Commun.* **2005**, *334*, 1365.
[38] A. V. Ougolkov, M. E. Fernandez-Zapico, D. N. Savoy, R. A. Urrutia, D. D. Billadeau, *Cancer Res.* **2005**, *65*, 2076.
[39] B. Aggarwal, *Cancer Cell* **2004**, *6*, 203.
[40] A. V. Ougolkov, D. D. Billadeau, *Future Oncol.* **2006**, *2*, 91.
[41] W. H. Robert, *Nature* **1975**, *258*, 487.
[42] T. Mosmann, *J. Immunol. Methods* **1983**, *65*, 55.
[43] CLC bio, *Molegro Virtual Docker User Manual, MVD 2012.5.5 for Windows, Linux, and Mac OS X*, *Molegro*—A CLC bio company 2012.

SUPPORTING INFORMATION

Additional supporting information may be found online in the Supporting Information section.

How to cite this article: Mokenapelli S, Thalari G, Vadiyaala N, et al. Synthesis, cytotoxicity, and molecular docking of substituted 3-(2-methylbenzofuran-3-yl)-5-(phenoxymethyl)-1,2,4-oxadiazoles. *Arch Pharm.* 2020;e2000006. https://doi.org/10.1002/ardp.202000006